New Journal of Physics
The open-access journal for physics

# Origin of the surface-state band-splitting in ultrathin Bi films: from a Rashba effect to a parity effect

**T Hirahara[1,9], K Miyamoto[2], A Kimura[2], Y Niinuma[1], G Bihlmayer[3], E V Chulkov[4,5], T Nagao[6], I Matsuda[7], S Qiao[8], K Shimada[8], H Namatame[8], M Taniguchi[2,8] and S Hasegawa[1]**

[1] Department of Physics, University of Tokyo, 7-3-1 Hongo, Bunkyo-ku, Tokyo 113-0033, Japan
[2] Graduate School of Science, Hiroshima University, 1-3-1 Kagamiyama, Higashi-Hiroshima 739-8526, Japan
[3] Institut für Festkörperforschung, Forschungszentrum Jülich, D-52425 Jülich, Germany
[4] Donostia International Physics Center(DIPC), 20018 San Sebastián/Donostia, Spain
[5] Departamento de Física de Materiales, UPV/EHU, Apdo 1072, 20080 San Sebastián, Spain
[6] Nano System Functionality Center, National Institute for Materials Science, 1-1 Namiki, Tsukuba, Ibaraki 305-0044, Japan
[7] Institute for Solid State Physics, 5-1-5, Kashiwanoha, Kashiwa, Chiba 277-8581, Japan
[8] Hiroshima Synchrotron Radiation Center, Hiroshima University, 2-313 Kagamiyama, Higashi-Hiroshima 739-0046, Japan
E-mail: hirahara@surface.phys.s.u-tokyo.ac.jp

*New Journal of Physics* **10** (2008) 083038 (12pp)
Received 3 June 2008
Published 28 August 2008
Online at http://www.njp.org/
doi:10.1088/1367-2630/10/8/083038

**Abstract.** Following our previous work (Hirahara T *et al* 2007 *Phys. Rev.* B **76** 153305), we have performed spin- and angle-resolved photoemission measurements at ∼120 K on ultrathin Bi films grown on a Si substrate, focusing on the split surface-state bands near the Fermi level. We found clear experimental evidence that these states show Rashba-type spin-split behavior near $\bar{\Gamma}$, but the splitting is lost near $\bar{M}$ where they overlap with the bulk band projection. This can be explained as a change in the origin of the splitting from a Rashba effect to a parity effect as revealed by *ab initio* calculations.

[9] Author to whom any correspondence should be addressed.

**Contents**



## 1. Introduction

Symmetry in physics is one of the most important concepts. We learn in classical and quantum mechanics that the behavior of physical quantities is related to the symmetry of the system. For example, in a spatially homogeneous system (continuous translation symmetry), the momentum conservation law holds, and in a system that holds continuous time translation, it is known that the energy is conserved [1].

In solid state physics, we learn that symmetry and the band structure also have a close relationship with each other. At the Brillouin zone boundary, the electrons are Bragg-reflected and an energy gap develops between states that behave differently with respect to a symmetry operation; the parity of the wave function is the opposite [2]. Also, clean (001) surfaces of semiconductors have bands called the $\pi$ and $\pi^*$ bands that have different symmetry; one is a bonding state and the other is an anti-bonding state [3]. Similarly, if the structure of the system becomes asymmetric, the degeneracy of bands is lifted and this is sometimes very useful in determining the actual structure of the system. One example of this is the absence of degeneracy observed in high symmetry points for the Si(111) $\sqrt{3} \times \sqrt{3}$-Ag surface, which showed that the structure has a lower symmetry than previously believed [4]. Furthermore, as surface states are inherently structural inversion asymmetric (SIA) systems because one side is vacuum and the other is the internal crystal, there has been growing interest in the Rashba effect, which makes the band spin-split due to the spin–orbit interaction even for non-magnetic materials [5]. Usually in the non-magnetic bulk, time-reversal symmetry ($E(\vec{k}, \uparrow) = E(-\vec{k}, \downarrow)$) and space-inversion symmetry ($E(\vec{k}, \uparrow) = E(-\vec{k}, \uparrow)$) lead to the Kramers degeneracy ($E(\vec{k}, \uparrow) = E(\vec{k}, \downarrow)$). However at the crystal surface, due to the SIA in the surface-normal direction the degeneracy will be lifted. Many studies have been performed for clean metal surfaces [6]–[9] as well as surface overlayers showing a large splitting [10]–[13].

Because there are several origins for the band splitting as discussed above, it is sometimes difficult to identify the real physical meaning. The case of Mg(0001)/W(110) is one such example. Koitzsch *et al* [14] have reported that the splitting of Mg(0001) surface-state bands stems from a Rashba effect due to the strong spin–orbit coupling of the W substrate. Schiller *et al* reported on the same system but with a totally different interpretation. They said that due to the long penetration depth of the wave function, the surface state bands are reflected at the film/substrate interface and form states with even and odd symmetries with respect to the central layer of the Mg film (parity effect) [15]. Shikin and Rader have shown another work insisting that neither of the two can completely explain the observed data and the origin of the splitting is still controversial [16].

In this paper, we show another intriguing system of ultrathin Bi films grown on a Si substrate in which the metallic surface states were shown to be largely band-split due to the strong spin–orbit interaction [9, 18]. Utilizing the ability of spin- and angle-resolved photoemission spectroscopy (SRARPES) measurements to investigate the spin structure in a wide region of momentum–energy space, we show that the Rashba effect smoothly transforms into a parity effect with the change of the wavenumber. This fact is supported by *ab initio* calculations. The present finding shows an interesting interplay and crossover between the relativistic and quantum size effects.

## 2. Experimental and calculation methods

The measurements were performed in the SRARPES system at Hiroshima Synchrotron Radiation Center [20, 21]. The spectra were recorded at ∼120 K using unpolarized HeI$\alpha$ radiation (21.2 eV) with a compact Mott detector operating at 25 keV [22]. The angle between the incident photons and the analyzer was 50°. The angular resolution was ±1° and the energy resolution was 120 meV for the pass energy ($E_p$) of 6 eV and 70 meV for $E_p = 3$ eV. In our measurement geometry, we can obtain the in-plane spin polarization of the spin component perpendicular to the plane spanned by the two vectors directed along the light incidence and electron emission, as shown in figure 1(a). We define the spin direction as 'up' and 'down' with respect to this plane, which can also be thought as 'left' and 'right' with respect to $k$. The spin polarization $P$ is obtained from $P = \frac{1}{S_{\text{eff}}}\frac{I_L - I_R}{I_L + I_R}$, where $I_L$ and $I_R$ are the measured intensities of the left and right detectors, and $S_{\text{eff}} = 0.128$ is the Sherman function. The spin-up and spin-down spectra are obtained by $I^{\uparrow,\downarrow} = (I_L + I_R)(1 \pm P)/2$. Epitaxial Bi(001) films (for our film orientation we use hexagonal notation Bi(001) which is Bi(111) in rhombohedral notation) were grown by the method described before [18, 23, 24]. The film thickness in the present measurement was 7 BL (bilayers, 1 BL = $1.14 \times 10^{15}$ atoms cm$^{-2}$, 0.39 nm thick).

The calculations have been performed using the full-potential linearized augmented plane wave (FLAPW) method in film geometry as implemented in the FLEUR program [25]. The method is based on the density functional theory in the local density approximation for the description of exchange–correlation potential. The details can be found in [9]. All the calculations shown in this paper were done for a 7 BL free-standing Bi slab.

## 3. Results and discussion

First, we summarize our earlier findings and also assign the possible spin orientation for the surface-state bands of Bi(001) [18]. Figure 1(b) shows the schematic drawing of the Fermi surface composed of the surface states reported in [18, 23]. The actual band dispersion along the $\bar{\Gamma}$–$\bar{M}$-direction measured by spin-integrated ARPES can be found in figure 1(c). Bismuth surface-state bands were reported to show spin–orbit splitting from *ab initio* calculations [9] and scanning tunneling spectroscopy measurements [19], and furthermore we found indication of surface states in a Bi(001) film actually being spin-split in our earlier SRARPES measurements [26]. The two-dimensional free electron gas Rashba split bands are parabolas shifted in the wavenumber direction with two concentric circles for the Fermi surface [17]. Because of the complex band structure of bulk Bi, the surface-state bands in the present case do not follow this behavior except for small k-vectors, but this splitting was also termed

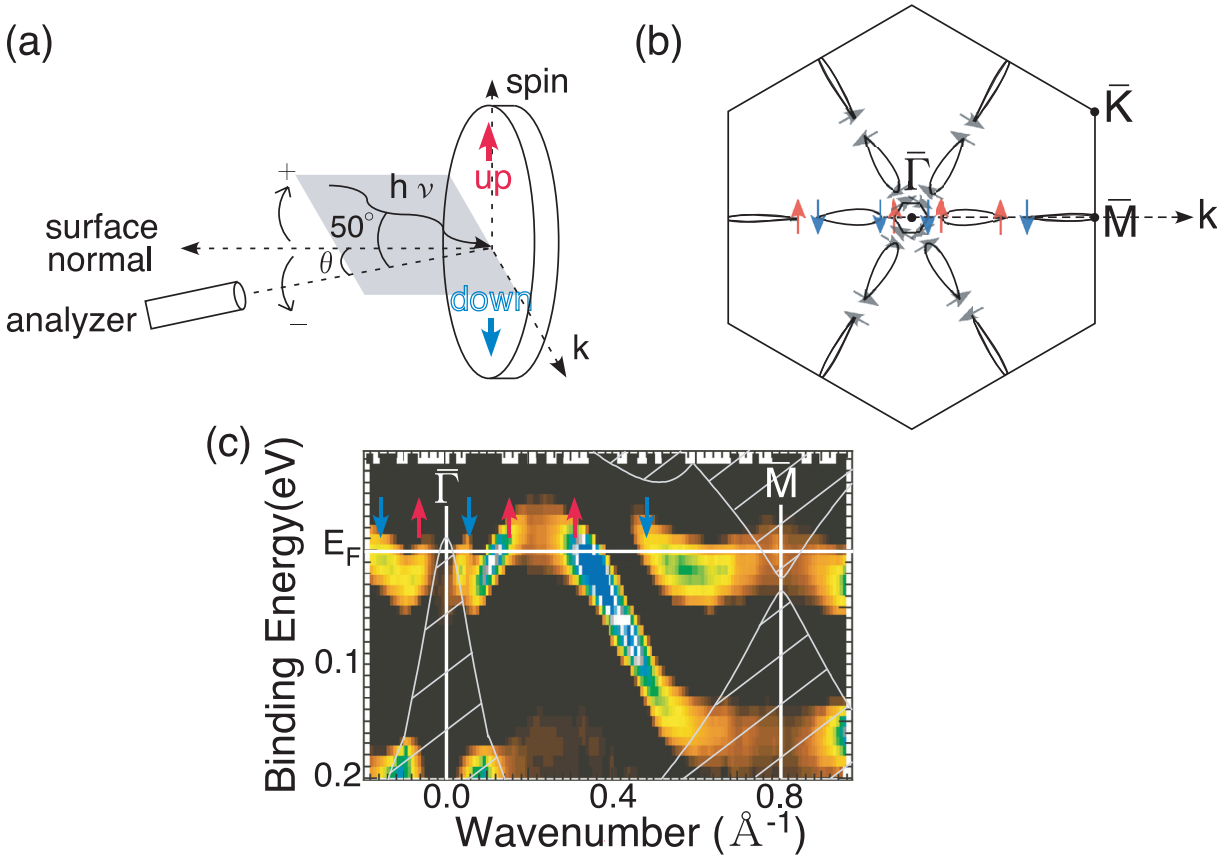


**Figure 1.** (a) Schematic illustration of the experimental setup. (b) Schematic drawing of the Fermi surface of Bi(001) ultrathin films [18] made up of surface states with the spin orientation assigned according to the Rashba model [17]. (c) The band structure of the surface state of a 17 BL ultrathin Bi(001) film in the vicinity of $E_F$ along the $\bar{\Gamma}$–$\bar{M}$-direction measured by non-spin-resolved ARPES [18]. The shaded area represents the bulk band projection [27]. The spin orientation shown in (b) is also indicated.

Rashba-type spin–orbit splitting to distinguish from an atomic spin–orbit splitting [9]. The most remarkable difference between figure 1(c) and the ideal Rashba-type behavior of the bands is the absence of a band crossing at the $\bar{M}$ point. This arises from the combination of the time-reversal and translational ($E(\vec{k}+\vec{G},\uparrow) = E(\vec{k},\uparrow)$) symmetries and the two bands should be degenerate at $\bar{\Gamma}$ and $\bar{M}$. However, we obviously see that the splitting is present throughout $\bar{\Gamma}$–$\bar{M}$ although the situation is not so clear at the $\bar{\Gamma}$ point due to the interference with quantum well states (QWSs). In an ideal Rashba-split band the inversion symmetry is assumed to be broken. But in the present case, the surface-state bands gradually change their character to QWSs near $\bar{M}$ whose electronic wave function spreads out throughout the entire thickness of the film. As a consequence, these states become 'electronically' inversion symmetric and result in the modification of the band topology as well as the spin-splitting [18, 26]. Concerning the spin orientation, we have assigned the spin orientation in analogy to the ideal Rashba model [17], and the result is shown in figures 1(b) and (c) by the arrows. Although it is important to investigate the polarization of

all the spin components, we think that the spin orientation between the present case and the Rashba model is not so different. Therefore, we have investigated the spin-splitting of the spin component shown in figures 1(b) and (c) and this corresponds to the direction indicated in figure 1(a). In summary, we have previously found that the surface states of Bi(001) show band-splitting throughout the surface Brillouin zone. Although most of the features can be explained by the Rashba-type effect, there are other factors and this suggests a change in the origin of the observed splitting.

We now turn to our SRARPES measurement results. Figures 2(a) and (c) show the SRARPES spectra taken at the pass energy of 3 eV near the $\bar{\Gamma}$ point. Figures 2(b) and (d) show the corresponding spin polarization. It is worth noting that the spectral features are much clearer than those reported in [26] taken at room temperature. At large positive emission angles in figure 2(a), we see near $E_F$ a clear spin-up peak with a maximum spin polarization value of $\sim$+0.75. We believe that ideally it should be unity, but due to the finite resolution and the temperature effect, the peak broadens and the spin-polarization value becomes smaller than 1. This is also evidenced by the fact that the obtained spin-polarization value is smaller for the spectra at higher pass energy (not shown) and those taken at room temperature in [26]. It should be noted that for the Au(111) surface which is said to mimic an ideal two-dimensional Rashba-split band, the experimentally observed spin polarization value was also only 0.4 at most [7]. This strongly suggests that this spin component is the only one that is spin-polarized in our Bi case. This observation that the spin-polarization is smaller than unity may also be related to the penetration depth as will be discussed later. As this peak approaches $\bar{\Gamma}$, the polarization goes down to $\sim$+0.3 at 2.25° (0.08 Å$^{-1}$). As it goes even closer to the $\bar{\Gamma}$ point, it starts to disappear and at 1.25° (0.05 Å$^{-1}$), a spin-down peak appears and persists to 0.75° (0.03 Å$^{-1}$) with the spin polarization of $\sim -0.3$. This is a clear observation of the change of the spin-split branch near $\bar{\Gamma}$. Just at normal emission, the peaks get weak and are non-polarized. Going on to negative angles in figure 2(c), we observe a sharp spin-up peak at $-0.75°$ ($-0.03$ Å$^{-1}$). This peak disperses to the Fermi level as we go away from $\bar{\Gamma}$, and at $-1.75°$ (0.05 Å$^{-1}$), we can see both the spin-up (30 meV) and -down (70 meV) peaks resolved. The spin-down peak then disperses closer to $E_F$. Until this angle, the SRARPES spectra presented in figures 2(a) and (c) are consistent with the prediction of figures 1(b) and (c), showing a clear antisymmetric spin structure. However, at angles smaller than $-2.75°$ (0.10 Å$^{-1}$), we observe that although the spin polarization shows a small negative value, the spin-down peak does not show up very clearly and rather the spin-up peak is seen quite well. At present, we are not sure of the reason for this strange observation, but it may be related to the asymmetric configuration of the light incidence (figure 1(a)), which may cause unequivalent matrix element effects for positive and negative emission angles during the photoemission process. Relativistic one-step model calculations of the SRARPES may be able to reproduce this feature [28].

To visualize the change of the spin orientation near $E_F$ in the vicinity of $\bar{\Gamma}$ pronouncedly, we have made a spin polarization map from the polarization curves of figures 2(b) and (d) near $E_F$. Figure 2(e) shows the obtained result with the intensity scaling linearly from blue, white, to red as the polarization value changes from negative, zero, to positive as indicated by the color scale bar at the top. We obviously find a clear change in spin polarization from positive to negative as we approach $\bar{\Gamma}$ from positive wavenumbers. Passing through $\bar{\Gamma}$ and going to negative wavenumbers, the polarization again turns back to positive (red). When we go further to larger wavenumbers, the polarization becomes nearly zero or a very small negative value. This is related to the discussion above, a clear explanation is not available at the moment. Although we

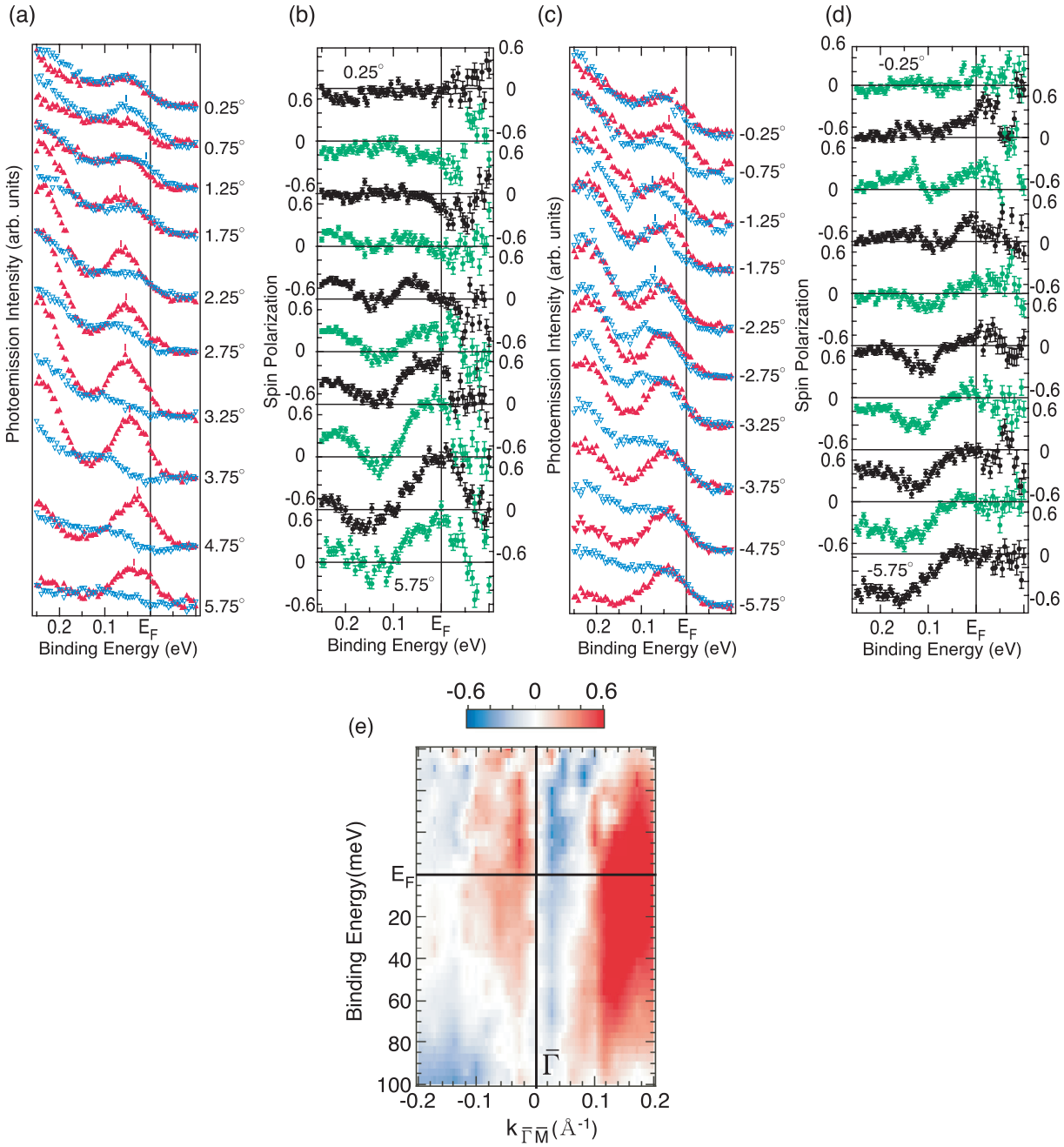


**Figure 2.** SRARPES spectra for the 7 BL Bi(001) film near normal emission taken at $E_p = 3$ eV, (a) and (c), and the respective spin-polarization curves, (b) and (d). (e) Image of the spin-polarization mapping deduced from the raw data of (b) and (d).

notice that the features are much sharper in figure 1(c), we can say that figure 2(e) is consistent with our spin assignment of the non-spin-resolved ARPES image shown in figure 1(c) and can be basically explained by the Rashba model as previously reported [19, 26]. Although the energy and angular resolutions of the present SRARPES system may not be so good, figure 2(e)

unequivocally shows that we can resolve the shallow spin-split states near $E_F$ even with the present resolution.

Now, let us discuss the results of SRARPES measurements at larger emission angles in the positive direction. Figure 3(a) shows the spin-integrated spectra from 8° ($k = 0.29$ Å$^{-1}$) to 29° ($k = 1.02$ Å$^{-1}$) for the 7 BL film. The data have been taken at $E_p = 6$ eV. We observe clear peak structures that correspond to surface states (filled circles) and QWSs (open triangles). The QWSs could not be observed clearly at room temperature in our previous report [26]. Figures 3(b) and (c) show the SRARPES spectra and the corresponding spin polarization curves, respectively. We notice that at 8°, a sharp spin-up peak is present just below $E_F$ shown by the red filled circle. As this peak disperses downwards approaching the $\bar{M}$ point, the peak width becomes broad. Furthermore, we can recognize that the spin-down spectra start to show peak features at the same energy as the spin-up spectra. This indicates that the spin-polarization is decreasing. Another spin-down peak emerges at 14° indicated by the blue open circle, which is the other surface-state branch just at $E_F$ near $\bar{M}$ in figure 1(c), and this state shows very small negative polarization, probably due to the effect of the Fermi–Dirac function and the limited resolution in our measurement. We also find that QWSs at higher binding energy are a bit positively polarized. At the $\bar{M}$ point (23° spectra), the spin-up and -down spectra overlap almost completely, meaning that there is practically no spin polarization for any state at this angle. As we pass $\bar{M}$, the shallow state near $E_F$ now shows a peak for the spin-up spectra, while the surface state with higher binding energy is negatively polarized. The next QWS also seems to be a bit negatively polarized. This shows that the spin structure is basically antisymmetric with respect to the $\bar{M}$ point.

Figure 3(d) shows the spin polarization dependence on the wavenumber for the two surface states close to $E_F$ indicated in figure 3(b). The red filled circles represent the state with higher binding energy (filled circles in figure 3(b)) and the blue open circles show the state closer to $E_F$ (open circles in figure 3(b)). The average of seven points around the peak energy ($\Delta E = \pm 35$ meV) was taken as the polarization value and the error bars show the standard deviation. For the states at higher $E_B$, we observe a systematic decrease of the spin polarization from $\sim$+0.37 at 0.29 Å$^{-1}$ to $\sim$0 at $\bar{M}$ and to $\sim -0.29$ at 1.01 Å$^{-1}$. The opposite trend can be seen for the states nearer to $E_F$, where the spin polarization increases from $\sim -0.08$ at 0.51 Å$^{-1}$ to $\sim$+0.03 at $\bar{M}$ and to $\sim$+0.08 at 0.92 Å$^{-1}$. Because the spin polarization values are quite small for the surface-state peaks closer to $E_F$, we do see some scattering of the data, but the general trend can be seen. As has been discussed, this reduction of spin polarization happens near the bulk projection. A similar observation has been reported for the W(110)-H surface [10], but the authors speculated that the change will be more abrupt showing a decrease just at the wavenumber that overlaps with the bulk projection rather than the gradual change actually observed. As discussed next, this trend is also consistent with the results of the first-principles calculations.

Figure 4(a) shows the spin-resolved energy band dispersion curves obtained from the present SRARPES measurement overlaid on the band dispersion image of the non-spin-resolved ARPES measurements. The solid red (empty blue) triangles pointing up (down) represent the spin-up (-down) states. The size of the markers for these states represents the magnitude of the spin polarization. The largest markers represent $\pm 0.75$ and as the size becomes small, the polarization becomes closer to zero. The states showing no significant spin polarization are represented by gray open circles. We have also plotted in figure 4(a) some points whose spectra we do not show here explicitly in figure 2 but have been reported in [26] (binding energy higher than 0.2 eV near the $\bar{\Gamma}$ point). Although we do see that near $E_F$, the peak

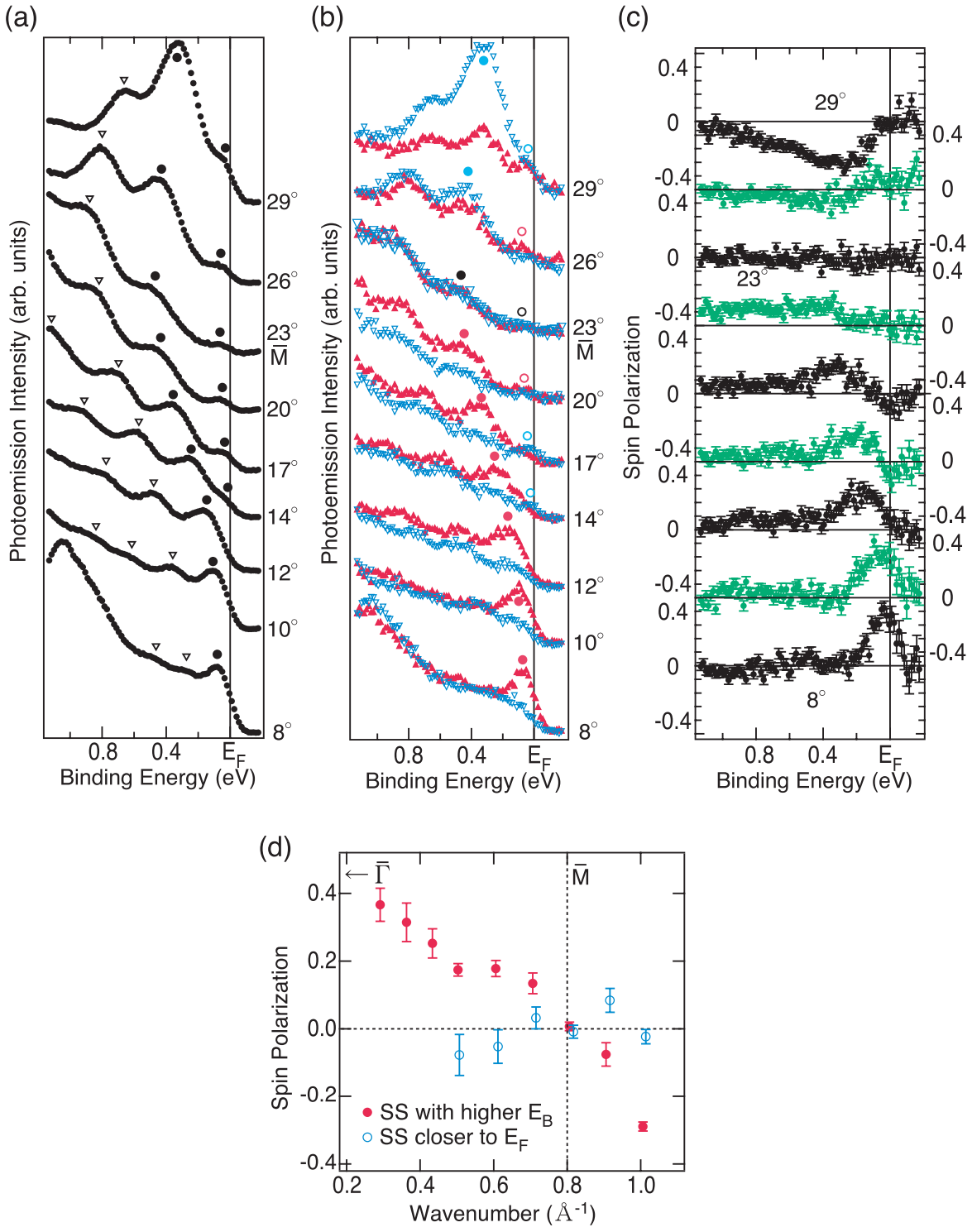


**Figure 3.** Spin-integrated (a) and spin-resolved (b) ARPES spectra of the 7 BL Bi(001) film near the $\bar{M}$ point. The solid circles (open triangles) in (a) show the peak positions of the surface states (QWSs). The filled and open circles in (b) correspond to the surface-state peaks at higher and lower binding energies, respectively. (c) The corresponding spin-polarization curves of (b). (d) Spin polarization dependence on the wavenumber along the $\bar{\Gamma}$–$\bar{M}$-direction.

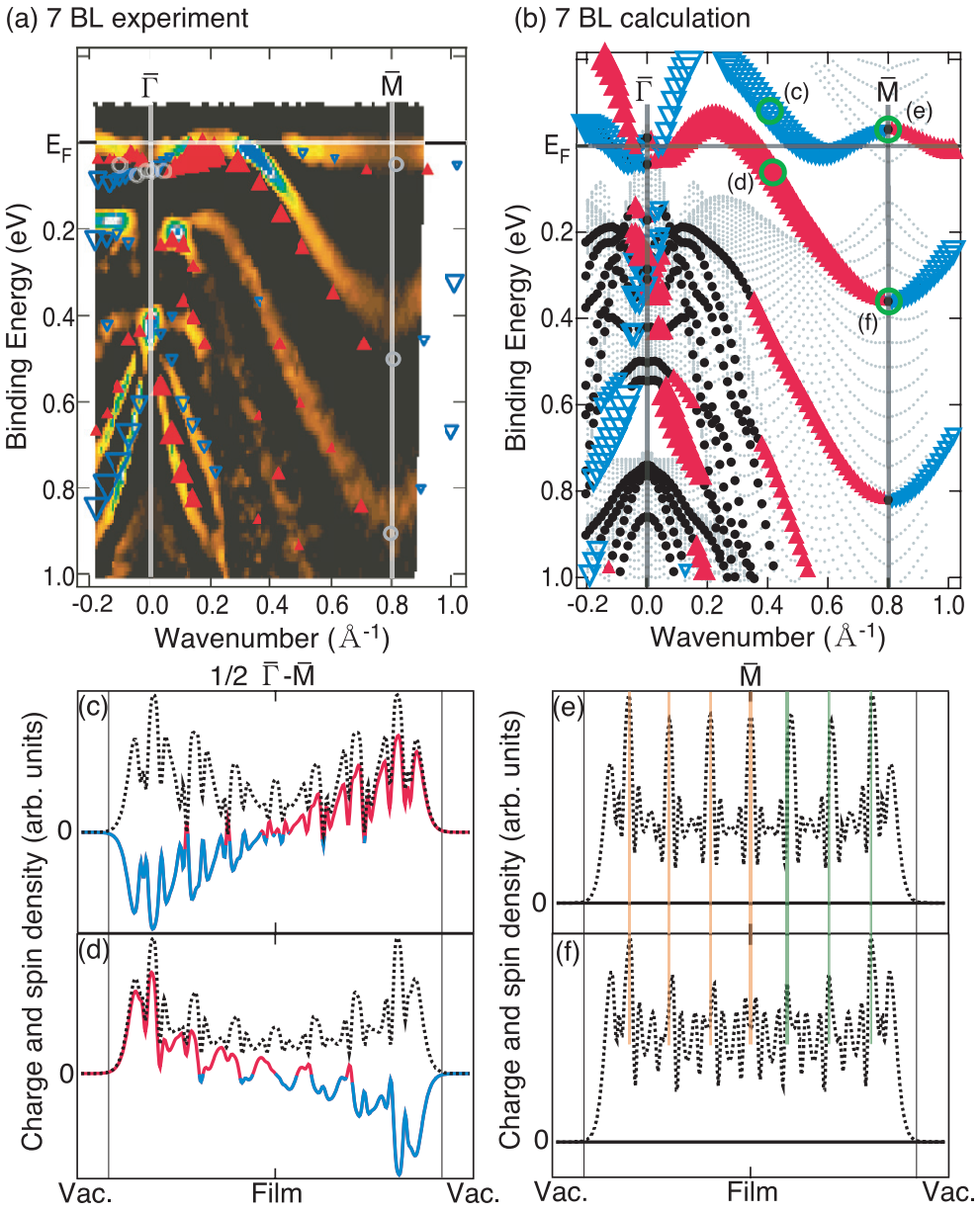


**Figure 4.** The spin-split band dispersion of the 7 BL Bi(001) films obtained from SRARPES overlaid on the dispersion obtained by non-spin-resolved ARPES (a), and the spin-polarized band structure of the *ab initio* calculations for free-standing 7 BL Bi slabs (b). The spin-up (-down) channels (in the calculation this refers to one particular surface of the film) are shown by the red solid triangles pointing up (blue empty triangles facing down) and the magnitude of the spin polarization is shown by the size of the markers (the largest ones represent $\pm 0.75$ for (a) and $\pm 0.94$ for (b), respectively). The non-polarized states are shown by gray open circles in (a) and filled black circles in (b). The small gray dots in (b) represent the bulk band projection. (c)–(f) The charge (dotted lines) and spin (solid lines) density distribution inside the film for the points indicated by circles in (b). The spin orientation is in-plane and perpendicular to the wave vector (figure 1(a)).

positions of the SRARPES measurements and the dispersions of the non-spin-resolved ARPES measurements are slightly different probably due to the limited resolution and the difference in the actual thickness, the features are almost the same. As has been discussed, the spin structure is basically antisymmetric with respect to both the $\bar{\Gamma}$ and the $\bar{\mathrm{M}}$ points even for the states inside the bulk band projection. The metallic surface-state bands are clearly spin-split near $\bar{\Gamma}$, but lose their spin-split property as they approach $\bar{\mathrm{M}}$.

We compare our experimental results with the *ab initio* calculations, depicted in figure 4(b)[10]. The gray dots show the bulk band projection. As discussed in [18, 26], the bands are spin-degenerate due to the conservation of the space-inversion symmetry if we consider the whole film. However, if we analyze the charge distribution inside the film and the in-plane spin component perpendicular to the wave vector (the spin component shown in figure 1), we can find local spin polarization[11]. The magnitude and the direction of the spin polarization is shown similar to the style of figure 4(a). The results of figure 4(b) can reproduce most features of figure 4(a) concerning the band topology as well as the qualitative spin-polarization dependence on the wavenumber. However, we do see slight discrepancies. For the spin-split surface states near the spin-orbit gap (0.4–0.9 eV near the $\bar{\Gamma}$ point) [26], in the experiment we have found that they show clear Rashba-type splitting behavior with antisymmetric spin structure. But this feature cannot be clearly seen in the calculation, as the upper and lower branches both seem to show the same polarization. This may be related to the mean free path of the photoemitted electrons as discussed below and further measurements for different film thicknesses as well as changing the incident photon energy will be interesting.

In order to give further consideration to the splitting of the metallic surface-state bands, we have explicitly plotted the spin and charge density distributions of these states in figures 4(c)–(f) which correspond to the points in $E$–$k$ space indicated by circles in figure 4(b). The solid lines show the spin density and the dotted lines show the charge density, respectively. Figures 4(c) and (d) are the plots for the pure surface states at the midpoint of $\bar{\Gamma}$–$\bar{\mathrm{M}}$ inside the bulk band gap, whereas figures 4(e) and (f) show the plots where the surface states have become QWSs at the $\bar{\mathrm{M}}$ point. We notice in figures 4(c) and (d) that the charge is distributed near the two film/vacuum interfaces and the spin polarization is the opposite for the two interfaces, i.e. one has positive polarization, whereas the other is negatively polarized. We also notice that the polarization at the same interface is the opposite between figures 4(c) and (d), mimicking the typical Rashba-splitting. On the contrary, for figures 4(e) and (f), the charge is distributed inside the whole film [18] and there is no spin-polarization. This can be understood as follows. At the middle of $\bar{\Gamma}$–$\bar{\mathrm{M}}$, the interaction between the top and bottom surfaces is very small such that the wave function of surface states has practically a node on the central layer of the film. We can make a linear combination of even and odd states, resulting in states located either on one side of the film or the other. One can consider this as a Rashba-type SO-splitting. On the other hand, near the $\bar{\mathrm{M}}$ point, because of the overlap with the bulk band, the wave function extends inside the film

[10] The calculations have been done in a similar manner to that shown in figure 3(b) of [18] but with the lattice constant taken as the experimental value in this case.

[11] Generally, 'spin-degeneracy' means that we have two (degenerate) states with opposite spin-polarization, while the term 'non-spin-polarization' can also refer to a single state $\psi$, where $\langle\psi|S_i|\psi\rangle = 0$ for all $i = x, y, z$, where $S$ is the spin-operator and the integration is over the full space. Thus, the terms 'spin-degenerate' and 'non-polarized' may not necessarily be used synonymously. In the present case, we can see from figures 4(c) and (d) that although the band is spin-degenerate, there is local spin-polarization spatially. The charge density distribution determines the local spin-polarization and this is the key point in our interesting findings.

and is reflected specularly at the film/substrate interface (the interaction at the top and bottom surfaces is quite strong) becoming QWSs. This results in a kind of even–odd splitting with a different symmetry with respect to the film center and this produces energetically separated bands at the $\bar{M}$ point. As discussed above, in the simple Rashba effect the two surface-state bands should cross each other at this point and therefore we can say that the spin property at the $\bar{M}$ point is dominated by the parity effect. It can be seen in figures 4(e) and (f) that the center of the film is an antinode for (e), whereas it seems to be a node in (f). The positions of the antinodes inside the film differ between (e) and (f) as shown by the solid orange and green lines. The splitting observed here at $\bar{M}$ seems to have no relation to the Rashba effect and therefore the states become non spin-polarized. The present experimental findings suggest that although the nature of the splitting concerning the spin polarization is completely different between the Rashba and the parity effects, they seem to connect quite smoothly. We can say that we have observed a novel and intriguing interplay of the Rashba and quantum size effects.

## 4. Conclusions

In summary, we have provided a new insight into the origin of the band splitting observed in metallic surface states on ultrathin Bi(001) films utilizing state-of-art SRARPES measurements and first-principles calculations. The Rashba effect plays the dominant role where the surface states are located in the bulk band gap but changes gradually into a parity effect due to quantum confinement where they start to overlap with the bulk projection. This demonstrates that band-splitting due to different symmetry-breakings with completely different characteristics can be smoothly jointed and suggests an intriguing crossover between relativistic and quantum size effects.

## Acknowledgments

We thank T Kadono, R Nishimura and K Kanomaru for their help during the measurements. This work has been supported by Grants-In-Aid from the Japanese Society for the Promotion of Science.

## References

[1] Schiff L I 1949 *Quantum Mechanics* (New York: McGraw-Hill)
[2] Kittel C 2005 *Introduction to Solid State Physics* (New York: Wiley)
[3] Nakatsuji K, Takagi Y, Komori F, Kusuhara H and Ishii A 2005 *Phys. Rev.* B **72** 241308
[4] Matsuda I *et al* 2003 *Phys. Rev.* B **68** 085407
[5] Rashba E I 1960 *Sov. Phys. Solid State* **2** 1109
[6] Lashell S, McDougall B A and Jensen E 1996 *Phys. Rev. Lett.* **77** 3419
[7] Hoesch M, Muntwiller M, Petrov V N, Hengsberger M, Patthey L, Shi M, Falub M, Greber T and Osterwalder J 2004 *Phys. Rev.* B **69** 241401
[8] Sugawara K, Sato T, Souma S, Takahashi T, Arai M and Sasaki T 2006 *Phys. Rev. Lett.* **96** 046411
[9] Koroteev Y M, Bihlmayer G, Gayone J E, Chulkov E V, Blügel S, Echenique P M and Hofmann P 2004 *Phys. Rev. Lett.* **93** 046403
[10] Hochstrasser M, Tobin J G, Rotenberg E and Kevan S D 2002 *Phys. Rev. Lett.* **89** 216802

[11] Ast C R, Henk J, Ernst A, Moreschini L, Falub M C, Pacilé D, Bruno P, Kern K and Grioni M 2007 *Phys. Rev. Lett.* **98** 186807
[12] Shikin A M, Varykhalov A, Prudnikova G V, Usachov D, Adamchuk V K, Yamada Y, Riley J D and Rader O 2008 *Phys. Rev. Lett.* **100** 057601
[13] Premper J, Trautmann M, Henk J and Bruno P 2007 *Phys. Rev.* B **76** 073310
[14] Koitzsch C, Battaglia C, Clerc F, Despont L, Garnier M G and Aebi P 2005 *Phys. Rev. Lett.* **95** 126401
[15] Schiller F, Keyling R, Chulkov E V and Ortega J E 2005 *Phys. Rev. Lett.* **95** 126402
[16] Shikin A M and Rader O 2007 *Phys. Rev.* B **76** 073407
[17] Winkler R 2003 *Spin–Orbit Coupling Effects in Two-Dimensional Electron and Hole Systems* (Berlin: Springer)
[18] Hirahara T, Nagao T, Matsuda I, Bihlmayer G, Chulkov E V, Koroteev Y M, Echenique P M, Saito M and Hasegawa S 2006 *Phys. Rev. Lett.* **97** 146803
[19] Pascual J I *et al* 2004 *Phys. Rev. Lett.* **93** 196802
[20] Iori K, Miyamoto K, Narita H, Sakamoto K, Qiao S, Kimura A, Shimada K, Namatame H and Taniguchi M 2005 *J. Elecron Spectrosc. Relat. Phenom.* **144–147** 997
[21] Iori K, Miyamoto K, Narita H, Sakamoto K, Kimura A, Qiao S, Shimada K, Namatame H and Taniguchi M 2006 *Rev. Sci. Instrum.* **77** 013101
[22] Qiao S, Kimura A, Harasawa A, Sawada M, Chung J G and Kakizaki A 1997 *Rev. Sci. Instrum.* **68** 4390
[23] Hirahara T, Nagao T, Matsuda I, Bihlmayer G, Chulkov E V, Koroteev Y M and Hasegawa S 2007 *Phys. Rev.* B **75** 035422
[24] Nagao T, Sadowski J T, Saito M, Yaginuma S, Fujikawa Y, Kogure T, Ohno T, Hasegawa Y, Hasegawa S and Sakurai T 2004 *Phys. Rev. Lett.* **93** 105501
[25] http://www.flapw.de
[26] Hirahara T *et al* 2007 *Phys. Rev.* B **76** 153305
[27] Liu Y and Allen R 1995 *Phys. Rev.* B **52** 1566
[28] Henk J, Hoesch M, Osterwalder J, Ernst A and Bruno P 2004 *J. Phys.: Condens. Matter* **16** 7581